COMPARISON OF LANDING REGIONS AT THE SOUTHERN LUNAR POLAR TERRAIN FOR WATER ICE ACCESS.

A. Kereszturi[1,2], S. J. Boazman[2], D. Heather[2], R. Tomka[2,3,2], and T. Warren[4], [1] Konkoly Thege Miklos Astronomical Institute, Research Centre for Astronomy and Earth Sciences, Hungary. (kereszturi.akos@csfk.org); [2]ESTEC, ESA, Noordwijk, Netherlands; [3]Geographical Institute, Research Centre for Astronomy and Earth Sciences, Hungary; [4]Atmospheric, Oceanic and Planetary Physics Department, Univ. of Oxford, Oxford, UK; [5]CSFK, MTA Centre of Excellence, Budapest, Konkoly Thege Miklós út 15-17., H-1121, Hungary.

Introduction: A critical point in landing site selection that the various datasets being used have different spatial resolution, and they also contain different level and type of uncertainties. One strategy to decrease this effect is to select larger areas than the landing ellipse, here four such area are evaluated.

Locations are surveyed at the southern lunar polar region, where H_2O might be present in the top 1 m of the regolith (Hayne et al 2015, Fisher et al. 2017, Li et al. 2018), where solar powered in-situ drilling payload, like PROSPECT (Heather et al. 2022a,b) could work. Operations require solar illumination for power, but at the same time the temperature (and related solar illumination) needs to be low to support ice stability.

Despite these difficulties, several upcoming missions will target such locations, thus four regions of them are evaluated here. Besides having elevated probability of H_2O in the shallow subsurface, the approach presented in this work supports drilling-oriented payloads and forms part of a larger landing site assessment study (Boazman et al, 2022).

Methods: Datasets, including topographical and thermal datasets were overlain and jointly interpreted. For evaluation of surface morphology, WAC and NAC images were analyzed (Chin et al. 2007, Tooley et al. 2010) and co-registered to LOLA based topographic data (Smith et al. 2010).

Subsurface temperature modelling has been completed according to King et al. (2020) using the Oxford 3D model to estimate possible ice occurrence locations. Terrains were selected where the modelled temperature is <125 K at 1 m depth, the surface is illuminated >30 % of time, and the slope angle is <15°. Unfortunately, above 75° S latitude, very few areas exist where solar illumination is >40 % with the current resolution of datasets.

Results: There are several scattered/fragmented areas that fulfil the selection criteria. These are not considered here but will be targeted by a next step, however it is possible to identify four moderately large areas, where such ideal terrain units are next to each other with slopes that are safe and accessible for landing process, and temperature is low enough at 1 m depth. Four such areas were considered, see in Figure 1.

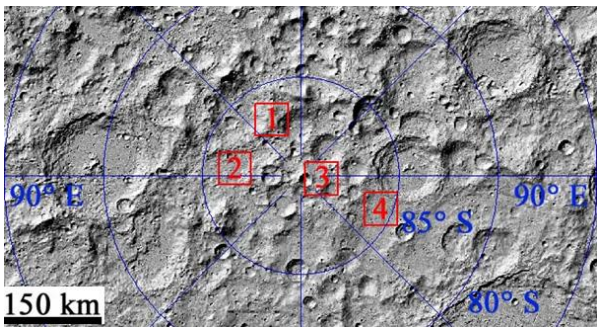

Figure 1. Locations of the region of interests (encircled with red) in the south polar region.

The four candidate areas (columns) can be seen below with magnified insets in Figure 2. Different lines of ihe insets show Sun visibility in percent (A), Earth visibility in percent (B), temperature below 1 m at the surface in K (C), temperature at the surface in K (D), slope in degrees (E), hillshade (F), water equivalent hydrogen in percent up to 0.54 in grayscale (with areas covered with black also less than 30 % in sun and Earth visibility) (G). Numerical values of the four candidate areas are summarized in Table 1. Areas with higher WEH values are suggestive of the presence of shallow surface ice.

The last two columns show required accuracy for safe landing with landing ellipse maximal sizes to gain a first insight into the required landing accuracy: the small landing circle covers an area with Earth and Sun visibility greater than 30 %, temperature below 125 K at 1 m depth and slope angle below 8°. In the large landing circle ~80 % of the area fulfils these criteria not the whole terrain, of course up to the spatial resolution of the used data. An example is indicated for target area no. 2 below in Figure 3.

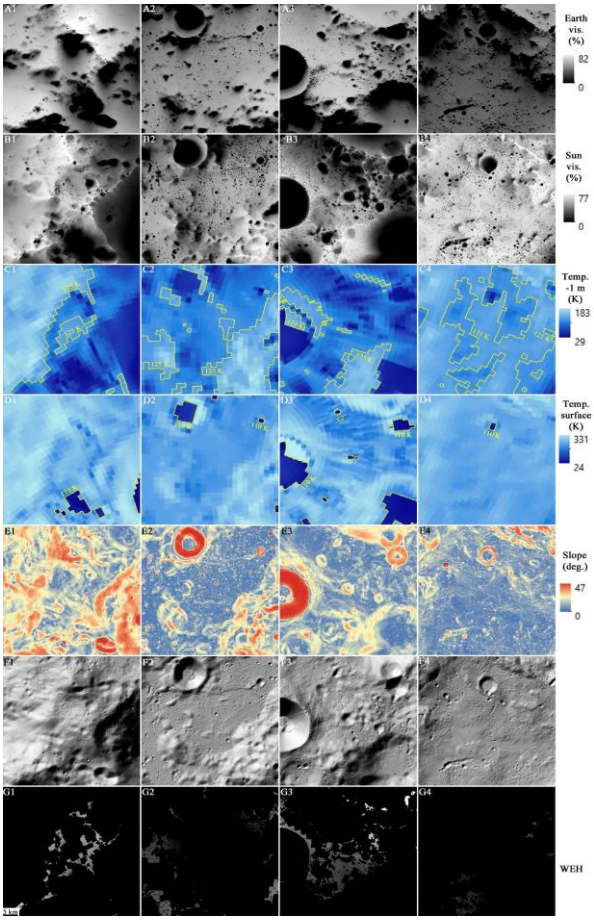

Figure 2. Magnified insets of the four candidate areas of Figure 1. Mapkey can be seen at right.

Summary: The joint evaluation of the landing site criteria showed there are almost no locations where surface ice might exist (<110 K) outside PSRs, but there are locations where solar illumination is ephemerally available, and the temperature is low enough at 1 m depth to support the long-term presence of ice. However large differences exist regarding the solar illumination with very few potential areas at 40 % but much more at 30 % illumination over time. Maximal diameter for safe and scientifically relevant landing ellipse sizes are around 0.5-1 km diameter, while larger ellipses around 2-4 km could be identified containing <20 % of unfavorable locations. The limiting factor of spatial resolution might influence all these values. Evaluation of subsections at these regions will be presented.

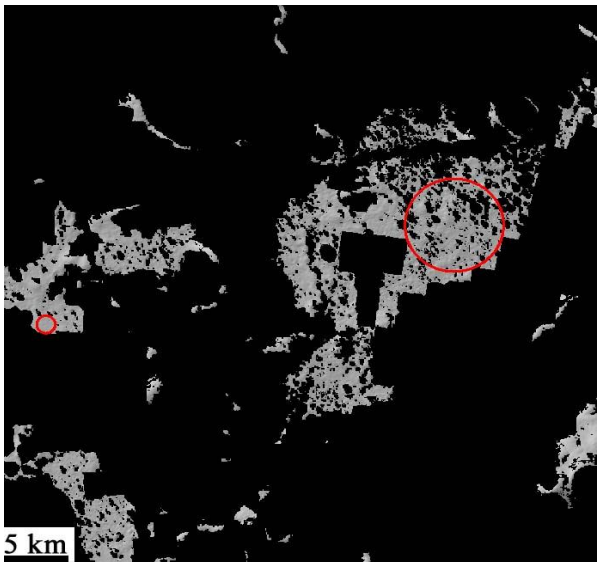

Figure 3. Potential landing sites at the region no. 2 marked with red circles.

Acknowledgement: This work was supported by the H82 POLICETECH project.

References: Boazman S. et al. 2022 *EPSC* #530; Chin, G. et al. 2007. *Space Sci. Rev.* 129, 391–419. Fisher E.A. et al. 2017. *Icarus* 292:74–85. Hayne P et al. 2015. *Icarus* 255:58–69. Heather D. et al. 2022. *EPSC* #533. Heather D. et al. 2022. 53rd *LPSC* #1825. King, O. et al. 2020. *Plan. Space Sci.* 182, 104790. Li S et al. 2018. *PNAS* 115(36):8907–8912. Mazarico et al. 2011. *Icarus* 211 1066. Sanin et al. 2017. *Icarus* 283, 20-30. Smith et al. 2010. *Space Sci. Rev.* 150, 209-241. Tooley et al. 2010. *Space Sci. Rev.* 150, 23–62.

Table 1. Numerical values of the four candidate regions.

No of reg	Center coordinates (°)	Area of T<110 K at surface	Area of T<125 K at 1 m depth	Area with slope <8° (and <15°)	Area of Earth and Sun visib. >30%	Area of Earth and Sun visib. >40%	Average (min. and max.) Water Equivalent Hydrogen (%)	Diam. small land. circle	Diam. large land. circle
1	-27.03, -86.75	3.29 %	57.08 %	27.64 (75.74)	35.68 %	10.63 %	0.24 (0.12-0.36)	719 m	1313 m
2	-83.91, -86.61	2.30 %	65.98 %	65.59 (90.50)	33.35 %	2.95 %	0.09 (0-0.27)	778 m	4147 m
3	94.11, -88.64	10.87 %	82.37 %	46.28 (79.18)	13.46 %	2.06 %	0.24 (0.07-0.46)	445 m	2624 m
4	112.56, -85.54	0.20 %	32.37 %	81.24 (96.16)	11.72 %	0.72 %	0.051 (0-0.18)	657 m	1537 m